Available online at www.scholarsresearchlibrary.com

Scholars Research Library

Archives of Physics Research, 2013, 4 (3):31-41
(http://scholarsresearchlibrary.com/archive.html)

Archives of Physics Research
Scholars Research Library
ISSN : 0976-0970
CODEN (USA): APRRC7

The scattering coefficient, extinction coefficient and single scattering albedo of soot in the radiative forcing of urban aerosols

D.O. Akpootu and S.B. Sharafa

Department of Physics, Usmanu Danfodiyo University, Sokoto, Nigeria.

ABSTRACT

Radiative forcing of aerosols is much more difficult to estimate than that of well-mixed gases due to the large spatial variability of aerosols and the lack of an adequate database on their radiative properties. In this paper, the optical depth, scattering coefficient, absorption coefficient, extinction coefficient and single scattering albedo were modeled using Optical Properties of Aerosols and Clouds (OPAC) by slightly altering the number densities of soot at visible wavelengths range of 0.25-1.00 μm for eight different relative humidities (RHs) (0, 50, 70, 80, 90, 95, 98 and 99%). The data obtained was used to estimate the radiative forcing (RF). The RF was observed to increase at all RHs given rise to positive RF when compared, as we moved from the first to the third models reflecting the dominance of warming effect. There are no noticeable changes in the scattering coefficient and extinction coefficient due to high percentage of volume mix ratio and mass mix ratio of water soluble when compared to the soot components; however, the single scattering albedo decreases with RHs attributing to a more absorbing aerosol. The regression analysis of the Ångström exponents and curvature which helps to determine the sizes of atmospheric particles was done using SPSS 16.0 Software, the analysis reveals the presence of fine mode particles.

Key words: Scattering coefficient, extinction coefficient, single scattering albedo, soot, radiative forcing, urban aerosols.

INTRODUCTION

Atmospheric aerosols are receiving more and more attention in research into climatic forcing [1-8]. Aerosols are also very important in the atmospheric correction of satellite remote sensing [9-10]. Sulfate aerosols, carbonaceous aerosols and mineral dust have a substantial climatic forcing effect in a cloud-free atmosphere, comparable with the effect of greenhouse gases [2-3]. Quantitatively, however, these estimates are still quite uncertain [3-4]. In particular, the lack of information about aerosol absorption is significant [3].

Radiative forcing due to aerosols is one of the largest sources of uncertainties in estimating anthropogenic climate perturbations [11]. Aerosols are produced by various sources that are highly inhomogeneous in both time and space [12-16]. Thus, estimating aerosol radiative forcing is much more complicated than estimating radiative forcing due to well-mixed greenhouse gases [11]. To estimate aerosol radiative forcing knowledge of the chemical composition is generally required. The data on aerosol physical and optical characteristics (such as aerosol optical depth and size distribution) are more readily available than data on aerosol chemical composition. This is because the determination of chemical composition requires dedicated field experiments and expensive instrumentation.

Absorption of solar radiation by soot, also known as black carbon (BC) particles is important in understanding the effects of atmospheric particles on climate. Particles with no absorption have a negative (cooling) forcing while particles with substantial absorption can have a positive (warming) forcing. As [17] noted, “Even though BC constitutes only a few percent of the aerosol mass, it can have a significant positive forcing. Jacobson recently found

that the magnitude of the direct radiative forcing from black carbon itself exceeds that due to CH_4 and may be the second most important component of global warming after CO_2 in terms of direct forcing [39].

Regional models that describe the spatial-temporal variability of atmospheric aerosol parameters are necessary to solve many radiative and climatic problems. An important area of study is the content of the main absorbing substance, soot (black carbon), in aerosol particles. Soot determines the nonselective absorption of radiation in the visible wavelength range by aerosol. It is an important radiative climatic factor because of its significant effect on the atmospheric transparency, albedo of clouds and snow cover [18].

Aerosol particles in the atmosphere are known to play critical roles in the global climate system by affecting the radiative balance of the Earth system [19]. Aerosols contribute to radiative forcing by the absorption and scattering of incoming solar radiation and outgoing thermal radiation from the Earth's surface [20]. An important quantity in the description of aerosol absorption and scattering is the single scattering albedo (SSA), ω_0. The extinction coefficient, γ, is defined as the sum of absorption coefficient, α and scattering coefficient, β [21] as

$$\gamma(\lambda) = \alpha(\lambda) + \beta(\lambda) \qquad (1)$$

The aerosol single scattering albedo, ω_0 is defined as the fraction of the aerosol light scattering over the extinction as

$$\omega_0 = \frac{\beta(\lambda)}{\gamma(\lambda)} \qquad (2)$$

and gives the fraction of extinction that is due to scattering. Aerosols with $\omega_0 = 1$ are pure scatterers and those with $\omega_0 < 1$ have an absorption component.

The aim of this paper is to calculate and analyze the effect of soot in the RF of urban aerosols at spectral range of 0.25 – 1.00 μm. The spectral behaviour of optical parameters analysed are the scattering coefficient, extinction coefficient and single scattering albedo which help in determining the nature of the aerosols. The Ångström exponents and curvatures were also analyzed to determine the fine and coarse mode particles along with the turbidity coefficient. We show that for situations where the absorption is due to soot, the single scattering albedo of the aerosol mixture should increase in wavelength and subsequently decrease with wavelength at certain spectral regions.

MATERIALS AND METHODS

The models extracted from OPAC are given in table 1.

Table 1: Compositions of aerosols types [22].

Components	Model 1	Model 2	Model 3
	No. density (cm^{-3})	No. density (cm^{-3})	No. density (cm^{-3})
Insoluble	1.50	1.50	1.50
water soluble	30,000.00	30,000.00	30,000.00
Soot	110,000.00	120,000.00	130,000.00
Total	140,001.50	150,001.50	160,001.50

The data used for the urban aerosols in this paper are derived from the Optical Properties of Aerosols and Clouds (OPAC) data set [22]. In this, a mixture of three components is used to describe Urban aerosols: a water soluble (WASO) components consist of scattering aerosols that are hygroscopic in nature, such as sulphates and nitrates present in anthropogenic pollution, water insoluble (INSO) and Soot.

To estimate the radiative forcing, we adopt the approach used by [23] where they show that the direct aerosol radiative forcing ΔF_R at the top of the atmosphere can be approximated by:

$$\Delta F_R = -\frac{S_0}{4} T_{atm}^2 (1 - N_{cloud}) 2\tau\{(1-a)^2 \beta\omega - 2a(1-\omega)\} \qquad (3)$$

where S_0 is the solar constant, T_{atm} is the transmittance of the atmosphere above the aerosol layer, N_{cloud} is the fraction of the sky covered by clouds, τ is the aerosol optical depth, ω is the average single scattering albedo of the aerosol layer, a is the albedo of the underlying surface and β is the fraction of radiation scattered by aerosol into the atmosphere [24]. The upscattering fraction is calculated using an approximate relation [25]

$$\beta = \frac{1}{2}(1 - g) \quad (4)$$

where g is the asymmetry parameter of the aerosol layer. The model parameters are assigned the following values: S_o=1368 Wm^{-2}, T_{atm}= 0.79 [24] N_{cloud} = 0.6 and the surface albedo and a = 0.22. although the model is simple, but, was used to provide reasonable estimates for the radiative forcing by both sulphate aerosols [1] and absorbing smoke aerosols [23].

The spectral behavior of the aerosols optical depth (τ). that expresses the spectral dependence of any of the optical parameters with the wavelength of light (λ) as inverse power law [26-27] is given by

$$\tau(\lambda) = \beta\lambda^{-\alpha} \quad (5)$$

The wavelength dependence of $\tau(\lambda)$ can be characterized by the Ångström parameter, which is a coefficient of the following regression:

$$ln\tau(\lambda) = -\alpha \ln(\lambda) + ln\beta \quad (6)$$

where β and α are the turbidity coefficient and Ångström exponent [28-29] α is related to the size distribution. The formula is derived on the premise that the extinction of solar radiation by aerosols is a continuous function of wavelength without selective bands or lines for scattering or absorption [30].

The Ångström exponent itself varies with wavelength, and a more precise empirical relationship between aerosol extinction and wavelength is obtained with a 2nd-order polynomial [31-38] as:

$$ln\tau(\lambda) = \alpha_2(ln\lambda)^2 + \alpha_1 ln\lambda + ln\beta \quad (7)$$

The coefficient α_2 accounts for "curvature" often observed in Sun photometry measurements. In case of negative curvature ($\alpha_2 < 0$) while positive curvature ($\alpha_2 > 0$). [32] Reported the existence of negative curvatures for fine mode aerosols and positive curvatures for significant contribution by coarse mode particles in the size distribution.

RESULTS AND DISCUSSION

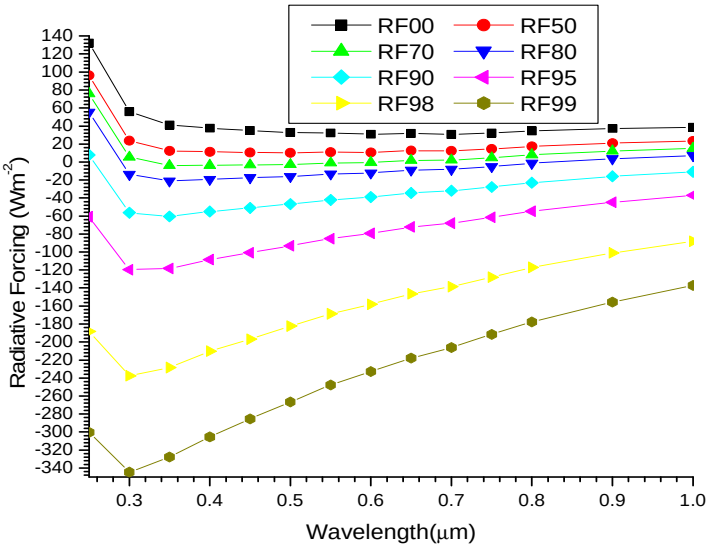

Figure 1a. A graph of radiative forcing against wavelength

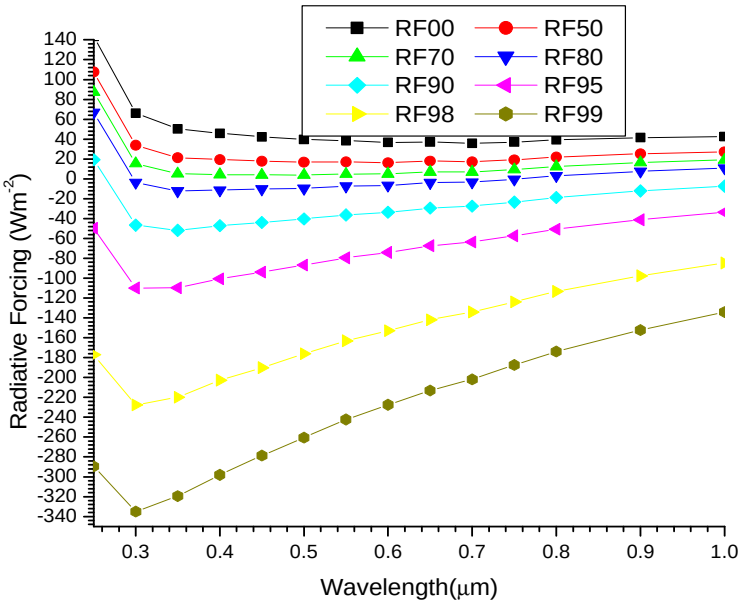

Figure 1b. A graph of radiative forcing against wavelength

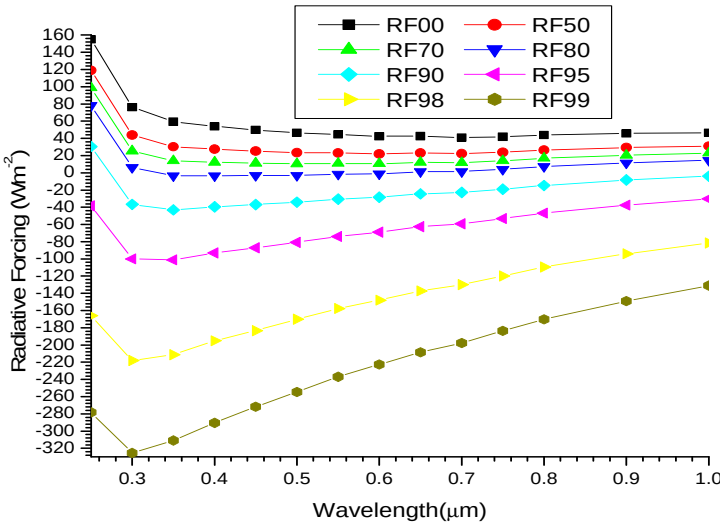

Figure 1c. A graph of radiative forcing against wavelength

In relation to wavelength, we observed that from 0-99% RHs in figure 1a, 1b and 1c as the soot increases shows that it is more dependent at shorter wavelengths with sharp fall at 0.25-0.3 μm, however, at 0% RH it becomes almost a straight line with very small positive slope. As the RHs increases from 50-99% RHs at spectral interval of 0.3-1.0 μm the value of the positive slope tends to increase as we moved from the first model to the third model. In relation to RHs; the RF increases with decrease in RHs as depicted in the figures. The overall effect is that there is a general increase in RF at all RHs as the soot increases when compared from figure 1a to figure 1c attributing to warming effect, this shows that soot has a high absorption coefficient.

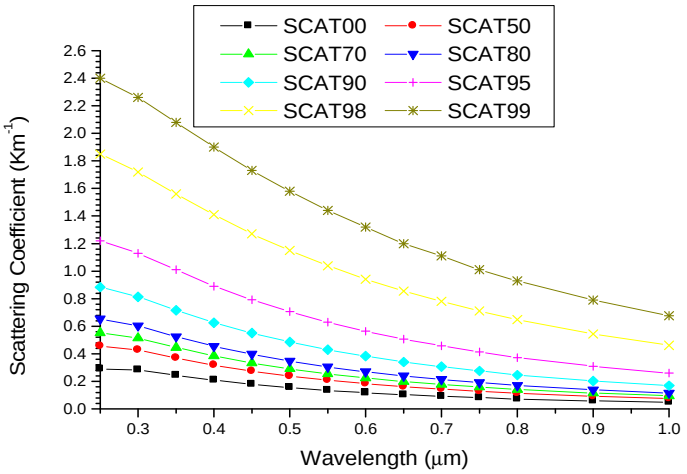

Figure 2a. A graph of scattering coefficient against wavelength

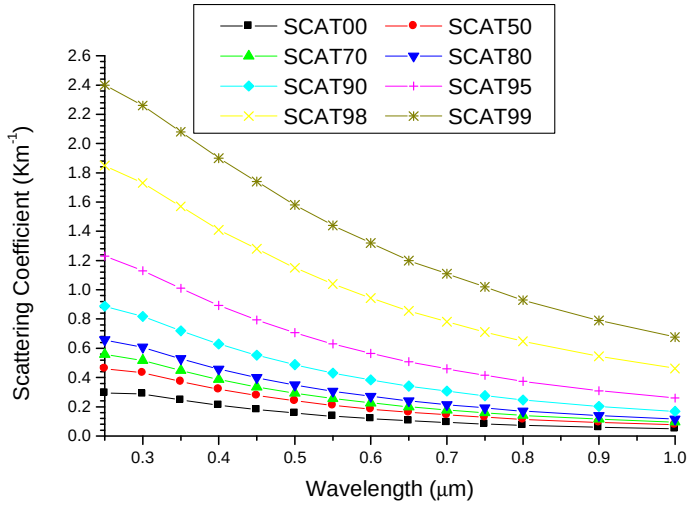

Figure 2b. A graph of scattering coefficient against wavelength

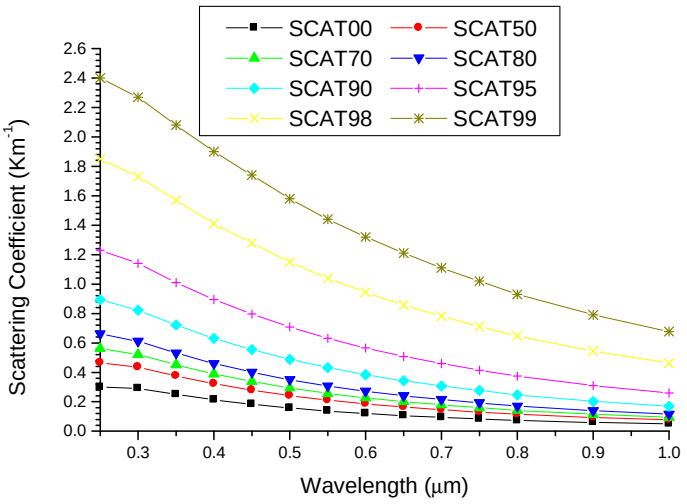

Figure 2c. A graph of scattering coefficient against wavelength

The scattering coefficients shown in Figure 2a to Figure 2c follow a relatively smooth decrease in wavelength at all RHs and can be approximated with power law wavelength dependence. It can be seen from the Figures that there is a relatively strong wavelength dependence of scattering coefficients at shorter wavelengths that gradually decreases towards longer wavelengths irrespective of the RH, attributing to the presence of both fine and coarse mode particles. The dominance of the higher concentration of the fine mode particles which are selective scatters enhances the irradiance scattering in shorter wavelengths only while the coarse mode particles provide similar contributions to the scattering coefficients at both wavelengths [40]. It also show that as a result of hygroscopic growth, smaller particles scatter more light at shorter wavelengths compared to bigger particles. The relation of scattering coefficients with RH is such that at the deliquescence point (90 to 99%) this growth with higher humidities increases substantially, making the process strongly nonlinear with relative humidities [41]. The overall effect in general shows that there are no noticeable changes in the scattering coefficient with RHs as we moved from the first model to the third model, this may be attributed to the high percentage of volume mix ratio and mass mix ratio of water soluble when compared to the soot components as shown in Table 5; since there is no observable increase in scattering coefficient the effect is that of warming the Earth's atmosphere.

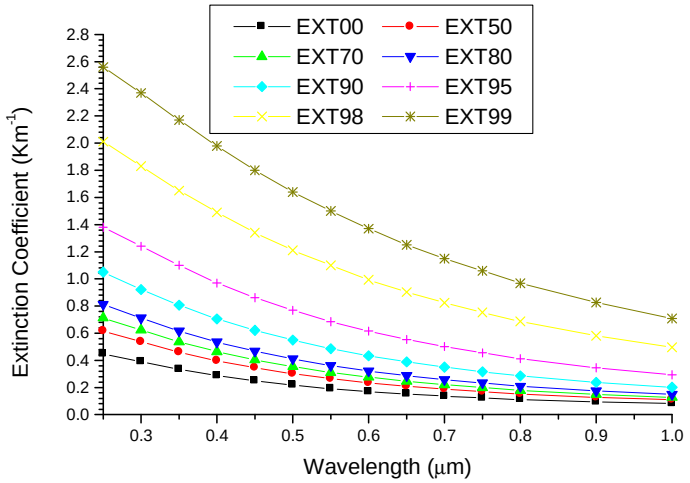

Figure 3a. A graph of extinction coefficient against wavelength

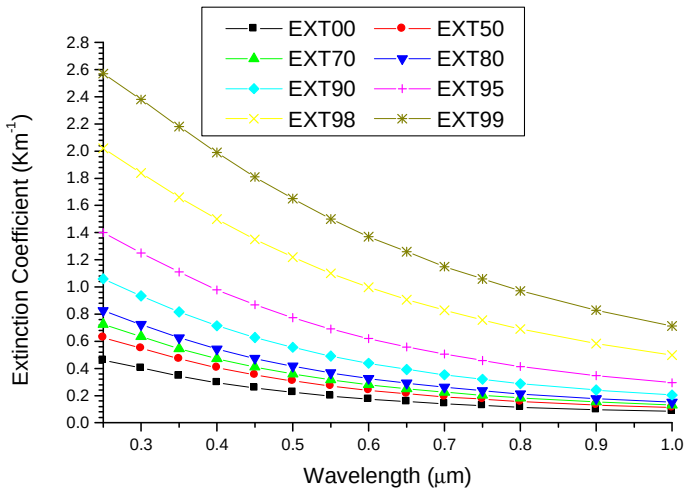

Figure 3b. A graph of extinction coefficient against wavelength

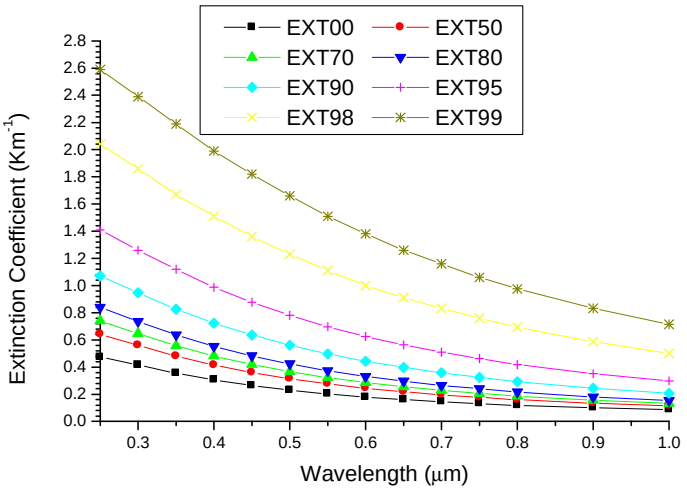

Figure 3c. A graph of extinction coefficient against wavelength

The extinction coefficient increases with increase in RHs. There is a relatively strong wavelength dependence of extinction coefficient at shorter wavelengths that gradually decreases towards the longer wavelength regardless of the RHs, attributing to the presence of both fine and coarse mode particles. Because the extinction coefficient is relatively constant with wavelength, the change in single scattering albedo is determined simply by the absorption coefficient spectral behavior. However, the single scattering albedo decreases as we moved from the first to the third models attributing to warming effect.

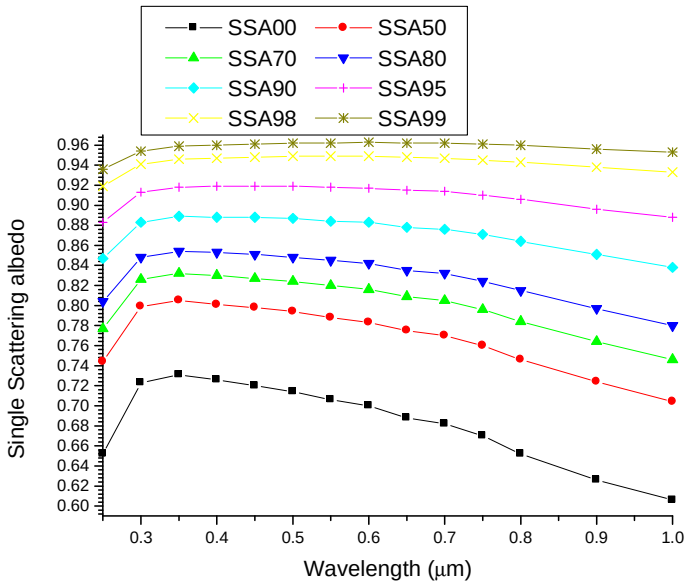

Figure 4a. A graph of single scattering albedo against wavelength

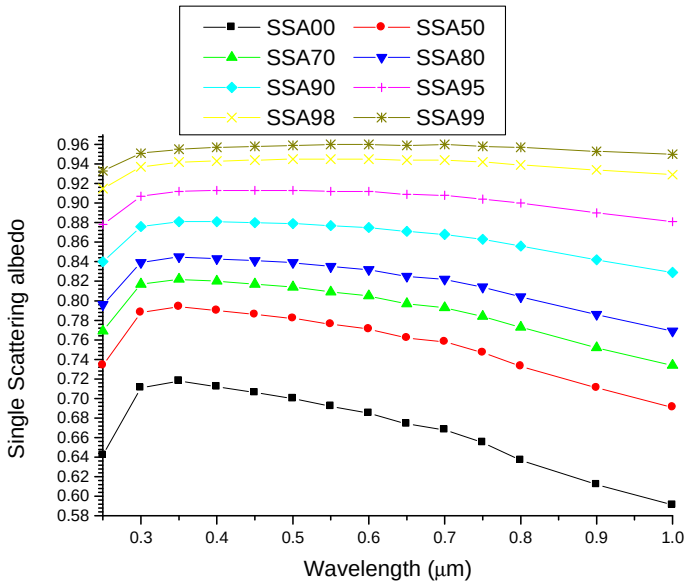

Figure 4b. A graph of single scattering albedo against wavelength

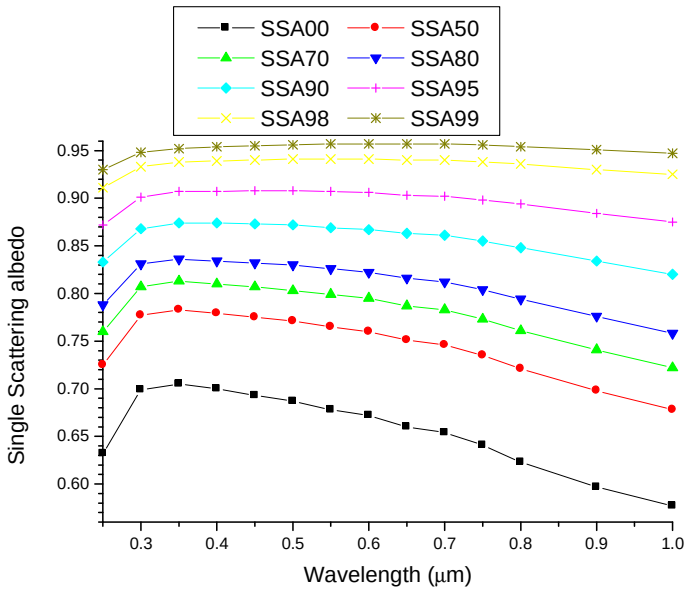

Figure 4c. A graph of single scattering albedo against wavelength

In relation to RHs we observed that from figure 4a to figure 4c the single scattering albedo, ω_0 increases with increase in RH as a result of hygroscopic growth. [42] reported that for urban industrial aerosols and biomass burning the ω_0 decreases with increasing wavelength, similarly [43] shown that the decrease in ω_0 with increasing wavelength is more as the RHs decreases, these effects are clearly observed in our figures. There is a sharp initial increase in ω_0 with wavelength at all RHs from 0.25-0.3 μm given rise to positive slope and subsequently decreases with wavelength at all RHs given rise to negative slope as from 0.3-1.0 μm. The overall effect shows that as soot increases from figure 4a to figure 4c there is a general decrease in ω_0 with RHs attributing that the aerosols has a high absorption coefficient reflecting warming effect.

Table 2: The results of α and α_2 for model 1 using equations (6) and (7) with SPSS 16.0

LINEAR				QUADRATIC			
RH(%)	R^2	α	β	R^2	α_1	α_2	β
0	0.99731	1.01207	2.31576	0.99815	-1.11236	-0.07357	2.26564
50	0.99602	1.07624	2.89341	0.99892	-1.27466	-0.14555	2.77083
70	0.99481	1.09212	3.27738	0.99917	-1.33907	-0.18115	3.10549
80	0.99350	1.09898	3.70573	0.99938	-1.38776	-0.21184	3.47947
90	0.99028	1.09243	4.82090	0.99964	-1.45523	-0.26614	4.45405
95	0.98582	1.05746	6.71730	0.99983	-1.48818	-0.31596	6.11485
98	0.97842	0.97475	10.94137	0.99995	-1.46880	-0.36242	9.82342
99	0.97236	0.90374	15.38190	0.99998	-1.42410	-0.38172	13.73121

Table 3: The results of α and α_2 for model 2 using equations (6) and (7) with SPSS 16.0

LINEAR				QUADRATIC			
RH(%)	R^2	α	β	R^2	α_1	α_2	β
0	0.99726	1.01868	2.36092	0.99813	-1.12123	-0.07522	2.30869
50	0.99602	1.08026	2.93870	0.99891	-1.27885	-0.14568	2.81410
70	0.99486	1.09529	3.32283	0.99916	-1.34138	-0.18052	3.14914
80	0.99352	1.10162	3.75116	0.99935	-1.39000	-0.21154	3.52244
90	0.99043	1.09465	4.86592	0.99963	-1.45508	-0.26440	4.49797
95	0.98598	1.05941	6.76225	0.99983	-1.48834	-0.31466	6.15817
98	0.97864	0.97662	10.98435	0.99995	-1.46895	-0.36116	9.86572
99	0.97264	0.90531	15.42577	0.99998	-1.42381	-0.38035	13.77596

Table 4: The results of α and α_2 for model 3 using equations (6) and (7) with SPSS 16.0

LINEAR				QUADRATIC			
RH(%)	R^2	α	β	R^2	α_1	α_2	β
0	0.99721	1.02499	2.40608	0.99811	-1.12987	-0.07694	2.35165
50	0.99602	1.08425	2.98367	0.99889	-1.28297	-0.14577	2.85709
70	0.99488	1.09861	3.36796	0.99914	-1.34423	-0.18018	3.19224
80	0.99358	1.10430	3.79662	0.99934	-1.39159	-0.21075	3.56597
90	0.99050	1.09665	4.91164	0.99962	-1.45611	-0.26369	4.54119
95	0.98606	1.06129	6.80781	0.99982	-1.48944	-0.31408	6.20073
98	0.97881	0.97827	11.02912	0.99995	-1.46933	-0.36023	9.90868
99	0.97289	0.90686	15.47032	0.99998	-1.42381	-0.37922	13.82041

Table 5: Analysis of volume mix ratio and mass mix ratio

		Model 1			Model 2			Model 3		
RH	COMP	NUMBER	VOL.MIX	MAS.MIX	NUMBER	VOL.MIX	MAS.MIX	NUMBER	VOL.MIX	MAS.MIX
[%]		[1/cm^3]	RATIO	RATIO	[1/cm^3]	RATIO	RATIO	[1/cm^3]	RATIO	RATIO
0	Inso	1.50E+00	0.38080	0.43190	1.50E+00	0.37600	0.42880	1.50E+00	0.37130	0.42570
	waso	3.00E+04	0.47830	0.48820	3.00E+04	0.47230	0.48470	3.00E+04	0.46640	0.48120
	Soot	1.10E+05	0.14090	0.07988	1.20E+05	0.15170	0.08651	1.30E+05	0.16230	0.09305
50	Inso	1.50E+00	0.26740	0.34870	1.50E+00	0.26500	0.34660	1.50E+00	0.26260	0.34460
	waso	3.00E+04	0.63380	0.58690	3.00E+04	0.62820	0.58350	3.00E+04	0.62260	0.58010
	Soot	1.10E+05	0.09883	0.06444	1.20E+05	0.10690	0.06989	1.30E+05	0.11470	0.07528
70	Inso	1.50E+00	0.22620	0.31110	1.50E+00	0.22450	0.30950	1.50E+00	0.22280	0.30790
	waso	3.00E+04	0.69020	0.63140	3.00E+04	0.68500	0.62810	3.00E+04	0.67990	0.62480
	Soot	1.10E+05	0.08360	0.05750	1.20E+05	0.09051	0.06240	1.30E+05	0.09732	0.06725
80	Inso	1.50E+00	0.19430	0.27910	1.50E+00	0.19300	0.27780	1.50E+00	0.19180	0.27650
	waso	3.00E+04	0.73390	0.66930	3.00E+04	0.72910	0.66620	3.00E+04	0.72440	0.66310
	Soot	1.10E+05	0.07181	0.05157	1.20E+05	0.07783	0.05600	1.30E+05	0.08377	0.06038
90	Inso	1.50E+00	0.14440	0.22410	1.50E+00	0.14370	0.22330	1.50E+00	0.14300	0.22240
	waso	3.00E+04	0.80220	0.73450	3.00E+04	0.79840	0.73170	3.00E+04	0.79450	0.72900
	Soot	1.10E+05	0.05337	0.04141	1.20E+05	0.05794	0.04500	1.30E+05	0.06246	0.04857
95	Inso	1.50E+00	0.10260	0.17030	1.50E+00	0.10230	0.16980	1.50E+00	0.10190	0.16930
	waso	3.00E+04	0.85940	0.79830	3.00E+04	0.85650	0.79600	3.00E+04	0.85350	0.79380
	Soot	1.10E+05	0.03793	0.03146	1.20E+05	0.04124	0.03422	1.30E+05	0.04452	0.03697
98	Inso	1.50E+00	0.06416	0.11380	1.50E+00	0.06402	0.11350	1.50E+00	0.06389	0.11330
	waso	3.00E+04	0.91210	0.86520	3.00E+04	0.91020	0.86360	3.00E+04	0.90820	0.86190
	Soot	1.10E+05	0.02371	0.02102	1.20E+05	0.02581	0.02289	1.30E+05	0.02790	0.02475
99	Inso	1.50E+00	0.04664	0.08531	1.50E+00	0.04657	0.08519	1.50E+00	0.04650	0.08507
	waso	3.00E+04	0.93610	0.89890	3.00E+04	0.93470	0.89760	3.00E+04	0.93320	0.89640
	Soot	1.10E+05	0.01724	0.01576	1.20E+05	0.01878	0.01717	1.30E+05	0.02031	0.01858

Various authors [30,32-33] reported that positive values of Ångström exponent α are characteristics of fine-mode-dominated aerosols size distributions while near zero and negative values are characteristics of dominant coarse-

mode or bi-modal size distributions, with coarse-mode aerosols having significant magnitude. Comparing Tables 2, 3 and 4. The Ångström exponents, α reflects the dominance of fine mode particles at all RHs which is verified by the curvature, α_2 at the linear and quadratic part of the regression analysis. The α increases from 0-80% RHs, decreases from 90-95% RHs, increases at 98% RH and subsequently decreases at 99% RH. The α_2 increases in magnitude from 0-99% RHs. The analysis further show that the turbidity, β increases with increase in RHs from 0-99% RHs in both the linear and quadratic part of the regression analysis indicating that the urban aerosols are associated with a relatively hazy atmosphere. The overall effect reveals the presence of fine mode particles or that the fine mode particles are dominant comparable to the coarse mode particles. [44] Reported that atmospheric aerosols are rarely mono modal, therefore, they are composed of poly dispersed aerosols.

CONCLUSION

Analysis of the results showed that RF (warming) increases at all RHs. Because extinction coefficient is relatively constant with wavelength, the change in single scattering albedo, $\omega_0$is determined simply by the absorption coefficient spectral behavior, though, there is an overall decrease in ω_0 with RHs indicating a more absorbing aerosols reflecting warming effect of the Earth's atmosphere. The values of the Ångström exponents, α and curvatures, α_2 indicates the dominance of fine mode particles which shows that hygroscopic growth has more effect on the fine mode particles than the coarse mode particles at spectral range of 0.25-1.00 μm and that is what is responsible for the radiative warming. However, we expect a decrease in scattering coefficient, but it shows no variation from the first to the third model, this may be attributed to the high percentage of volume mix ratio and mass mix ratio of water soluble when compared to the soot aerosol particles.

In this study, we have shown that for atmospheric aerosol mixtures where the absorption is due to soot, the single scattering albedo, ω_0 should increase with wavelength in the region of 0.25-0.30 μm and decrease with wavelength in the region of 0.30-1.00 μm. This is agreement with that reported by [45] where they show that ω_0 decreases with wavelength in the region of 0.30-1.00 μm, though, our results shows that there is an initial increase in ω_0 with wavelength in the region of 0.25-0.30 μm and in contrasts with the increase in the single scattering albedo, ω_0 with wavelength in the range of 0.30-1.00 μm for mineralogical dusts [46-47] and indicates the need for more careful measurements of the wavelength dependence of the aerosol absorption and single scattering albedo, ω_0. our analysis shows that the decrease in ω_0 with increasing wavelength is more as the RHs decreases, this is in agreement with that reported by [43]. We calculated the ω_0 for the analysis of soot and obtained values ranging from 0.630 to 0.936 at spectral range of 0.25-1.00 μm.

REFERENCES

[1] R. J. Charlson, S. E. Schwartz, J. M. Hales, R. D. Cess, J. A. Coakley, J. E. Hansen, and D. J. Hoffmann, *Science*, **1992,** 255, 423-430.
[2] J.T. Kiehl, and B.P. Briegleb, *Science* **1993,** 260, 311-314.
[3] J.E. Penner, R.J. Charlson, J.M. Hales, N.S. Laulainen, R. Novakov, J. Ogren, L.F. Radke, S.E. Schwartz, and L. Travis, *Bull. Am. Meteorol. Soc* **1994,** 75, 375-400.
[4] K.E. Taylor, and J.E Penner, *Nature* **1994,** 369, 734-737.
[5] N.G. Androvana, F.Y. Rozanov, M.E. Schlesinger, and G.L. Stenchikov, *Journal of Geophysical Research*, **1999,** 104(D14), 16807-16816.
[6] L. Bengtsson, E. Roeckner, and M. Stendel, *Journal of Geophysical Research*, **1999,** 104(D4), 3865-3878.
[7] P. Hignett, J.P. Taylor, P.N. Francis, and M.D. Glew, *Journal of Geophysical Research*, **1999,** 104(D2), 2279-2287.
[8] S. Menon, J. Hansen, L. Nazarenko, and Y. Luo, *Science*, **2002,** 297, 2250-2253.
[9] Y.J. Kaufman, D. Tanre, H.R. Gordon, T. Nakajima, J. Lenoble, R. Frouin, H. Grassl, B.M. Herman, M.D. King, and P. M. Teillet, *Journal of Geophysical Research*, **1997,** 102, 16815-16830.
[10] H.R. Gordon, *Journal of Geophysical Research*, **1997,** 102(D14), 17081-17106.
[11] J.T. Houghton, L.G. Meira Filho, J.P. Bruce, H. Lee, B.A. Callander, and E.F. Haites, Climate change 1994: Radiative forcing of climate change and an evaluation of the IPCC. Cambridge University Press, **1995,** 347 pp.
[12] G.E. Shaw, J.A. Regan, and B.M. Herman, *J. Appl. Meteor*, **1973,** 12, 374-380.
[13] J.M. Prospero, *Rev. Geophys. Space Physics*, **1983,** 21, 1607-1629.
[14] T.S. Bates, B.J. Hubert, J.L. Gras, F.B. Griffiths, and P.A. Durkee, *Journal of Geophysical Research*, **1998,** 103, 16297-16318.
[15] P.B. Russell, P.V. Hobbs, and L.L. Stowe, *Journal of Geophysical Research*, **1999,** 104, 2213-2222.
[16] P.K. Quinn, *Tellus*, 2000, 52B, 239-257.

[17] J. Heintzenberg, R.J. Charlson, A.D. Clarke, C. Liousse, V. Ramaswamy, K.P. Shine, M. Wendish, and G. Helas, *Beitr. Phys. Atmosph*, **1997,** 70, 249-263.
[18] M.V. Panchenko, V.S. Kozlov, and S.A. Terpugova, Institute of Atmospheric Optics, Tomsk, Russia **2001,** pp 1-5.
[19] IPCC, *Climate change*, **2007**.
[20] P. Chylek, and J.A. Coakley, *Science*, **1974,** 183, 75-77.
[21] H. Moosmuller, R. K. Chakrabarty, and W. P. Arnott, *A review, J. Quant Spectrosc. R*, **2009,** 110, 844-878.
[22] M. Hess, P. Koepke, and I. Schult, Optical Properties of Aerosols and Clouds. American Meteorology Society. **1998,** 831-844.
[23] P. Chylek, and J. Wong, *Geophysical Research Letters*, **1995,** 22, 929-931.
[24] J. E. Penner, R. E. Dickinson,and C. A. O'Neill, *Science*, **1992,** 256, 1432-1434.
[25] C. Sagan, and J. Pollack, *Journal of Geophysical Research*, **1967,** 72, 469-477.
[26] A. Ångström, *Geografiska Annaler*, **1929,** 11, 156-166.
[27] A. Ångström, *Tellus*, **1961,** 13(2), 214-223.
[28] K. N. Liou, An introduction to Atmospheric Radiation 2nd ed. Academic, San Diego, California. **2002**
[29] N. T. O'Neill, and A. Royer, *Appl. Opt*, **1993,** 32, 1642-1645.
[30] R. R. Ranjan, H. P. Joshi, and K. N. Iyer, *Aerosol and Air Quality Research*, **2007,** 7, 33-45
[31] M. King and D. Byrne, *Journal of Geophysical Research*, **1976,** 33, 3251-3254.
[32] T. F. Eck, B. N. Holben, J. S. Reid, O. Dubovik, A. Smirnov, N. T. O'Neill, I. Slutsker, and S. Kinne, *Journal of Geophysical Research*, **1999,** 104, 333-349.
[33] T. F. Eck, B. N. Holben, O. Dubovic, A. Smirnov, I. Slutsker, J. M. Lobert, and V. Ramanathan, *Journal of Geophysical Research*, **2001a,** 106, 28,555-28,566.
[34] T. F. Eck, B. N. Holben, D. E. Ward, O. Dubovik, J.S. Reid, A. Smirnov, M.M. Mukelabai, N.C. Hsu, N.T. O'Neill, and V. Ramanathan, *Journal of Geophysical Research*, **2001b,** 106, 3425-3448.
[35] T. F. Eck, B. N. Holben, D. E. Ward, O. Dubovik, J. S. Reid, A. Smirnov, M. M. Mukelabai, N. C. Hsu, N. T. O'Neill, and I. Slutsker, *Journal of Geophysical Research*, **2003,** 106, 3425-2448.
[36] Y. Kaufman, *Journal of Geophysical Research*, **1993,** 98 (D2), 2677-2692.
[37] N. T. O'Neill, O. Dubovik, and T. F. Eck, *Appl. Opt* , **2001,** 40 (15), 2368-2375.
[38] N. T. O'Neill, T. F. Eck, A. Smirnov, B. N. Holben, and S. Thulasiraman, *Journal of Geophysical Research*, **2003,** 108 (D17), 4559.
[39] M.Z. Jacobson, *Letters to Nature*, **2001,** 409, 695-697.
[40] G. L. Schuster, O. Dubovik, and B. N. Holben, *Journal of Geophysical Research*, **2006,** 111, 72-97.
[41] J. W. Fitzgerald, *Journal of Applied Meteorology*, **1975,** 14, 1044-1049
[42] O. Dubovik, B. Holben, T. Eck, A. Smirnov, Y. Kaufman, M. King, D. Tanre, and I. Slutsker, *J. Atmos Sci*, **2002,** 59, 1135-1150.
[43] D.O. Akpootu, and M. Momoh, *Scholars Research Library*, **2013,** 5(2), 109-120.
[44] K. Whisby, *Atmospheric environment*, **1978,** 12, 135-140.
[45] R.W. Bergstrom, P.B. Russell, and P. Hignett, *Journal of Atmospheric Sciences*, **2000,** 1-19.
[46] I. Sokolik, and O.B. Toon, *Nature*, **1997,** 381, 681.
[47] I. Sokolik, and O.B. Toon, *Journal of Geophysical Reseach*, **1999,** 104, 9423-9444.